Collapsed Cores in Globular Clusters, Gauge-Boson Couplings, and AASTeX Examples

S. Djorgovski[1,2,3] and Ivan R. King[1]

Astronomy Department, University of California, Berkeley, CA 94720

C. D. Biemesderfer[4,5]

National Optical Astronomy Observatories, Tucson, AZ 85719

aastex-help@aas.org

and

R. J. Hanisch[5]

Space Telescope Science Institute, Baltimore, MD 21218

Received ⎯⎯⎯⎯⎯⎯⎯; accepted ⎯⎯⎯⎯⎯⎯⎯

Not to appear in Nonlearned J., 45.

---

[1]Visiting Astronomer, Cerro Tololo Inter-American Observatory. CTIO is operated by AURA, Inc. under contract to the National Science Foundation.

[2]Society of Fellows, Harvard University.

[3]present address: Center for Astrophysics, 60 Garden Street, Cambridge, MA 02138

[4]Visiting Programmer, Space Telescope Science Institute

[5]Patron, Alonso's Bar and Grill

ABSTRACT

This is a preliminary report on surface photometry of the major fraction of known globular clusters, to see which of them show the signs of a collapsed core. We also explore some diversionary mathematics and recreational tables.

Subject headings: globular clusters: general — globular clusters: individual(NGC 6397, NGC 6624, NGC 7078, Terzan 8

1. Introduction

A focal problem today in the dynamics of globular clusters is core collapse. It has been predicted by theory for decades (Hènon 1961; Lynden-Bell & Wood 1968; Spitzer 1985), but observation has been less alert to the phenomenon. For many years the central brightness peak in M15 (King 1975; Newell & O'Neil 1978) seemed a unique anomaly. Then Aurière (1982) suggested a central peak in NGC 6397, and a limited photographic survey of ours (Djorgovski & King 1984, Paper I) found three more cases, NGC 6624, NGC 7078, and Terzan 8), whose sharp center had often been remarked on (Canizares et al. 1978).

As an example of how the new AASTeX object tagging macros work, we will cite some of the "Superlative" objects mentioned in section 10 of Trimble's (1992) review of astrophysics in the year 1991. The youngest star yet found was IRAS 4 in NGC 1333. 70 Oph was found to be the longest period spectroscopic binary. The most massive white dwarf was GD 50, estimated at 1.2 solar masses. The first neutral hydrogen found in a globular cluster was NGC 2808 while the I Zw 18 retained the record for metal deficiency. However, another low metallicitity galaxy was UGC 4483 in the M 83 group. The largest redshift source in 1991 was found at z=4.897. Lastly, what paper would be complete without a mention of the Crab nebula!

2. Observations

All our observations were short direct exposures with CCD's. We also have a random *Chandra* data set ADS/Sa.ASCA#X/86008020 and a neat HST FOS spectrum that readers can access via the links in the electronic edition. Unfortunately this has nothing whatsoever to do with this research. At Lick Observatory we used a TI 500×500 chip and a GEC 575×385, on the 1-m Nickel reflector. The only filter available at Lick was red. At CTIO

we used a GEC 575×385, with B, V, and R filters, and an RCA 512×320, with U, B, V, R, and I filters, on the 1.5-m reflector. In the CTIO observations we tried to concentrate on the shortest practicable wavelengths; but faintness, reddening, and poor short-wavelength sensitivity often kept us from observing in U or even in B. All four cameras had scales of the order of 0.4 arcsec/pixel, and our field sizes were around 3 arcmin.

The CCD images are unfortunately not always suitable, for very poor clusters or for clusters with large cores. Since the latter are easily studied by other means, we augmented our own CCD profiles by collecting from the literature a number of star-count profiles (King et al. 1968; Peterson 1976; Harris & van den Bergh 1984; Ortolani et al. 1985), as well as photoelectric profiles (King 1966, 1975) and electronographic profiles (Kron et al. 1984). In a few cases we judged normality by eye estimates on one of the Sky Surveys.

3. Helicity Amplitudes

It has been realized that helicity amplitudes provide a convenient means for Feynman diagram[1] evaluations. These amplitude-level techniques are particularly convenient for calculations involving many Feynman diagrams, where the usual trace techniques for the amplitude squared becomes unwieldy. Our calculations use the helicity techniques developed by other authors (Hagiwara & Zeppenfeld 1986); we briefly summarize below.

---

[1]Footnotes can be inserted like this.

3.1.   Formalism

A tree-level amplitude in e^+e^- collisions can be expressed in terms of fermion strings of the form

$$\bar{v}(p_2, \sigma_2)P_{-\tau}\hat{a}_1\hat{a}_2\cdots\hat{a}_n u(p_1, \sigma_1), \tag{1}$$

where p and σ label the initial $e^\pm$ four-momenta and helicities ($\sigma = \pm 1$), $\hat{a}_i = a_i^\mu\gamma_\nu$ and $P_\tau = \frac{1}{2}(1 + \tau\gamma_5)$ is a chirality projection operator ($\tau = \pm 1$). The a_i^μ may be formed from particle four-momenta, gauge-boson polarization vectors or fermion strings with an uncontracted Lorentz index associated with final-state fermions.

In the chiral [E1] representation the γ matrices are expressed in terms of 2×2 Pauli matrices σ and the unit matrix 1 as

$$\gamma^\mu = \begin{pmatrix} 0 & \sigma_+^\mu \\ \sigma_-^\mu & 0 \end{pmatrix}, \gamma^5 = \begin{pmatrix} -1 & 0 \\ 0 & 1 \end{pmatrix},$$
$$\sigma_\pm^\mu = (\mathbf{1}, \pm\sigma),$$

giving

$$\hat{a} = \begin{pmatrix} 0 & (\hat{a})_+ \\ (\hat{a})_- & 0 \end{pmatrix}, (\hat{a})_\pm = a_\mu\sigma_\pm^\mu, \tag{2}$$

The spinors are expressed in terms of two-component Weyl spinors as

$$u = \begin{pmatrix} (u)_- \\ (u)_+ \end{pmatrix}, v = ((v)_+^\dagger, (v)_-^\dagger). \tag{3}$$

The Weyl spinors are given in terms of helicity eigenstates $\chi_\lambda(p)$ with $\lambda = \pm 1$ by

$$u(p, \lambda)_\pm = (E \pm \lambda|\mathbf{p}|)^{1/2}\chi_\lambda(p), \tag{4a}$$
$$v(p, \lambda)_\pm = \pm\lambda(E \mp \lambda|\mathbf{p}|)^{1/2}\chi_{-\lambda}(p) \tag{4b}$$

[E1]NOTE TO EDITOR: Figures 1 and 2 should appear side-by-side in print

4.   Floating material and so forth

Consider a task that computes profile parameters for a modified Lorentzian of the form

$$I = \frac{1}{1 + d_1^{P(1+d_2)}} \tag{5}$$

where

$$d_1 = \sqrt{\left(\frac{x_1}{R_{maj}}\right)^2 + \left(\frac{y_1}{R_{min}}\right)^2}$$

$$d_2 = \sqrt{\left(\frac{x_1}{PR_{maj}}\right)^2 + \left(\frac{y_1}{PR_{min}}\right)^2}$$

$$x_1 = (x - x_0)\cos\Theta + (y - y_0)\sin\Theta$$

$$y_1 = -(x - x_0)\sin\Theta + (y - y_0)\cos\Theta$$

In these expressions x_0, y_0 is the star center, and Θ is the angle with the x axis. Results of this task are shown in table 1. It is not clear how these sorts of analyses may affect determination of $M_\odot$, but the assumption is that the alternate results should be less than $90°$ out of phase with previous values. We have no observations of Ca II. Roughly $\frac{4}{5}$ of the electronically submitted abstracts for AAS meetings are error-free.

We are grateful to V. Barger, T. Han, and R. J. N. Phillips for doing the math in section 3.1. More information on the AASTeX macros package is available at http://www.aas.org/publications/aastex. For technical support, please write to aastex-help@aas.org.

Facilities: Nickel, HST (STIS), CXO (ASIS).

A.   Appendix material

Consider once again a task that computes profile parameters for a modified Lorentzian of the form

$$I = \frac{1}{1 + d_1^{P(1+d_2)}} \tag{A1}$$

where

$$d_1 = \frac{3}{4}\sqrt{\left(\frac{x_1}{R_{maj}}\right)^2 + \left(\frac{y_1}{R_{min}}\right)^2}$$

$$d_2 = \tfrac{3}{4}\sqrt{\left(\frac{x_1}{PR_{maj}}\right)^2 + \left(\frac{y_1}{PR_{min}}\right)^2} \tag{A2a}$$

$$x_1 = (x - x_0)\cos\Theta + (y - y_0)\sin\Theta \tag{A2b}$$

$$y_1 = -(x - x_0)\sin\Theta + (y - y_0)\cos\Theta \tag{A2c}$$

For completeness, here is one last equation.

$$e = mc^2 \tag{A3}$$

REFERENCES

Aurière, M. 1982, A&A, 109, 301

Canizares, C. R., Grindlay, J. E., Hiltner, W. A., Liller, W., & McClintock, J. E. 1978, ApJ, 224, 39

Djorgovski, S., & King, I. R. 1984, ApJ, 277, L49

Hagiwara, K., & Zeppenfeld, D. 1986, Nucl.Phys., 274, 1

Harris, W. E., & van den Bergh, S. 1984, AJ, 89, 1816

Hénon, M. 1961, Ann.d'Ap., 24, 369

Heiles, C. & Troland, T. H., 2003, ApJS, preprint doi:10.1086/381753

Kim, W.-T., Ostriker, E., & Stone, J. M., 2003, ApJ, 599, 1157

King, I. R. 1966, AJ, 71, 276

King, I. R. 1975, Dynamics of Stellar Systems, A. Hayli, Dordrecht: Reidel, 1975, 99

King, I. R., Hedemann, E., Hodge, S. M., & White, R. E. 1968, AJ, 73, 456

Kron, G. E., Hewitt, A. V., & Wasserman, L. H. 1984, PASP, 96, 198

Lynden-Bell, D., & Wood, R. 1968, MNRAS, 138, 495

Newell, E. B., & O'Neil, E. J. 1978, ApJS, 37, 27

Ortolani, S., Rosino, L., & Sandage, A. 1985, AJ, 90, 473

Peterson, C. J. 1976, AJ, 81, 617

Rudnick, G. et al., 2003, ApJ, 599, 847

Spitzer, L. 1985, Dynamics of Star Clusters, J. Goodman & P. Hut, Dordrecht: Reidel, 109

Treu, T. et al., 2003, ApJ, 591, 53

3C138
(L,B)=(187.4,−11.3)
TAU = [0.04, 0.25, 0.18, 0.06, 1.05, 0.41]
VLSR= [−21.5, −0.4, 1.7, 1.9, 6.4, 9.1]
FWHM= [3.5, 2.9, 1.8, 14.6, 2.3, 2.8]
B = [39.5, 10.6, 7.3, 13.0, 5.6, −5.6]
ΔB = [16.4, 3.1, 3.4, 26.9, 1.6, 2.2]

INSTRUMENTAL CONTRIBUTION

(LINEAR POL)/10
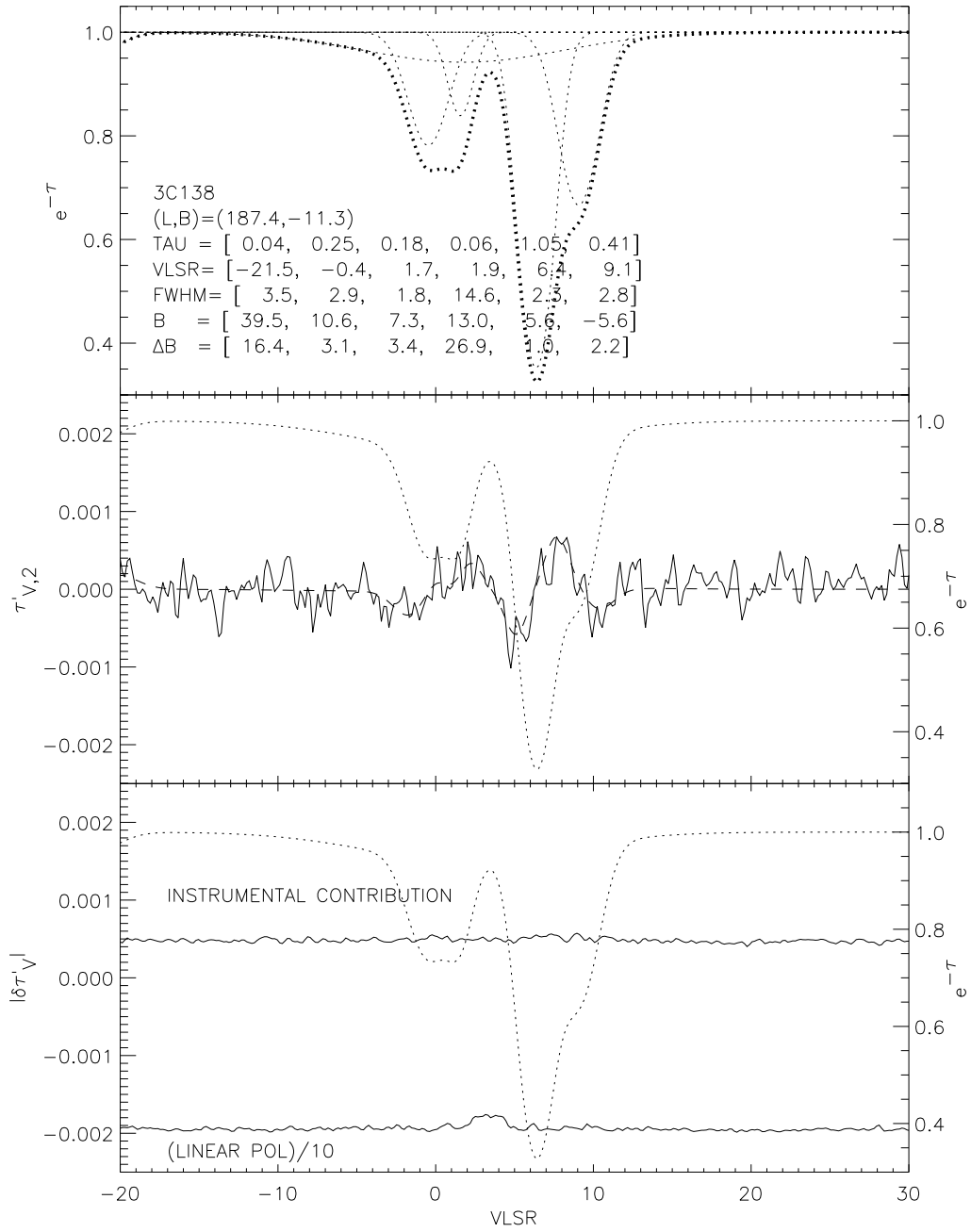
Fig. 1.— Derived spectra for 3C138 (see Heiles & Troland 2003). Plots for all sources are available in the electronic edition of *The Astrophysical Journal.*

Fig. 2.— A panel taken from Figure 2 of Rudnick et al. (2003). See the electronic edition of the Journal for a color version of this figure.
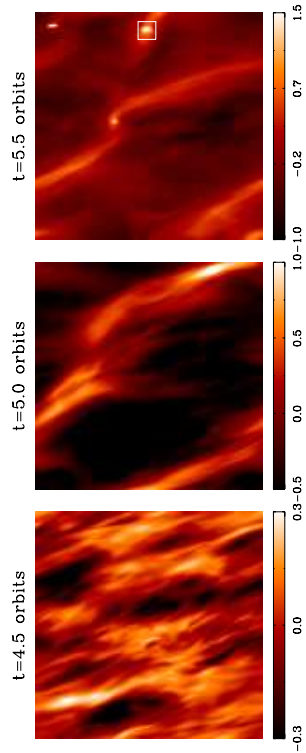
Fig. 3.— Animation still frame taken from Kim, Ostricker, & Stone (2003). This figure is also available as an mpeg animation in the electronic edition of the *Astrophysical Journal*.

Table 1.   Sample table taken from Treu et al. (2003)

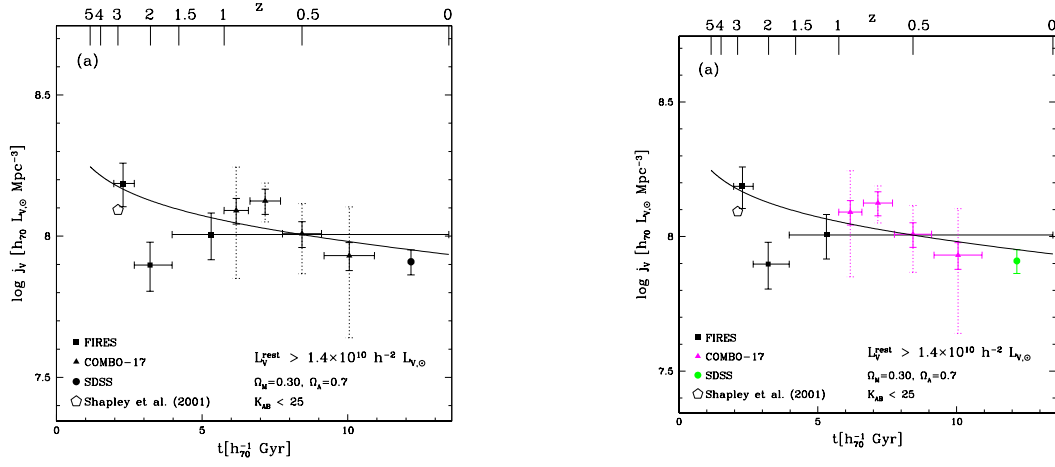| POS	chip	ID	X	Y	RA	DEC	IAU± δ IAU	IAP1± δ IAP1	IAP2 ± δ IAP2	star	E	Comment
0	2	1	1370.99	57.35	6.651120	17.131149	21.344±0.006	2 4.385±0.016	23.528±0.013	0.0	9	-
0	2	2	1476.62	8.03	6.651480	17.129572	21.641±0.005	2 3.141±0.007	22.007±0.004	0.0	9	-
0	2	3	1079.62	28.92	6.652430	17.135000	23.953±0.030	2 4.890±0.023	24.240±0.023	0.0	-	-
0	2	4	114.58	21.22	6.655560	17.148020	23.801±0.025	2 5.039±0.026	24.112±0.021	0.0	-	-
0	2	5	46.78	19.46	6.655800	17.148932	23.012±0.012	2 3.924±0.012	23.282±0.011	0.0	-	-
0	2	6	1441.84	16.16	6.651480	17.130072	24.393±0.045	2 6.099±0.062	25.119±0.049	0.0	-	-
0	2	7	205.43	3.96	6.655520	17.146742	24.424±0.032	2 5.028±0.025	24.597±0.027	0.0	-	-
0	2	8	1321.63	9.76	6.651950	17.131672	22.189±0.011	2 4.743±0.021	23.298±0.011	0.0	4	edge

Note. — Table 1 is published in its entirety in the electronic edition of the *Astrophysical Journal*. A portion is shown here for guidance regarding its form and content.

[a]Sample footnote for table 1 that was generated with the deluxetable environment

[b]Another sample footnote for table 1

Table 2: More terribly relevant tabular information.

Star	Height	d_x	d_y	n	χ^2	R_{maj}	R_{min}	P[a]	PR_{maj}	PR_{min}	Θ[b]
1	33472.5	-0.1	0.4	53	27.4	2.065	1.940	3.900	68.3	116.2	-27.639
2	27802.4	-0.3	-0.2	60	3.7	1.628	1.510	2.156	6.8	7.5	-26.764
3	29210.6	0.9	0.3	60	3.4	1.622	1.551	2.159	6.7	7.3	-40.272
4	32733.8	-1.2[c]	-0.5	41	54.8	2.282	2.156	4.313	117.4	78.2	-35.847
5	9607.4	-0.4	-0.4	60	1.4	1.669[c]	1.574	2.343	8.0	8.9	-33.417
6	31638.6	1.6	0.1	39	315.2	3.433	3.075	7.488	92.1	25.3	-12.052

[a]Sample footnote for table 2 that was generated with the LaTeX table environment

[b]Yet another sample footnote for table 2

[c]Another sample footnote for table 2

Note. — We can also attach a long-ish paragraph of explanatory material to a table.

– 14 –

Table 3.   Literature Data for Program Stars

Star	V	b−y	m$_1$	c$_1$	ref	T$_{\text{eff}}$	log g	v$_{\text{turb}}$	[Fe/H]	ref
HD 97	9.7	0.51	0.15	0.35	2	⋯	⋯	⋯	−1.50	2
						5015	⋯	⋯	−1.50	10
HD 2665	7.7	0.54	0.09	0.34	2	⋯	⋯	⋯	−2.30	2
						5000	2.50	2.4	−1.99	5
						5120	3.00	2.0	−1.69	7
						4980	⋯	⋯	−2.05	10
HD 4306	9.0	0.52	0.05	0.35	20, 2	⋯	⋯	⋯	−2.70	2
						5000	1.75	2.0	−2.70	13
						5000	1.50	1.8	−2.65	14
						4950	2.10	2.0	−2.92	8
						5000	2.25	2.0	−2.83	18
						⋯	⋯	⋯	−2.80	21
						4930	⋯	⋯	−2.45	10
HD 5426	9.6	0.50	0.08	0.34	2	⋯	⋯	⋯	−2.30	2
HD 6755	7.7	0.49	0.12	0.28	20, 2	⋯	⋯	⋯	−1.70	2
						5200	2.50	2.4	−1.56	5
						5260	3.00	2.7	−1.67	7
						⋯	⋯	⋯	−1.58	21
						5200	⋯	⋯	−1.80	10
						4600	⋯	⋯	−2.75	10
HD 94028	8.2	0.34	0.08	0.25	20	5795	4.00	⋯	−1.70	22

Table 3—Continued

Star	V	b−y	m_1	c_1	ref	T_{eff}	log g	v_{turb}	[Fe/H]	ref
						5860	⋯	⋯	−1.70	4
						5910	3.80	⋯	−1.76	15
						5800	⋯	⋯	−1.67	17
						5902	⋯	⋯	−1.50	11
						5900	⋯	⋯	−1.57	3
						⋯	⋯	⋯	−1.32	21
HD 97916	9.2	0.29	0.10	0.41	20	6125	4.00	⋯	−1.10	22
						6160	⋯	⋯	−1.39	3
						6240	3.70	⋯	−1.28	15
						5950	⋯	⋯	−1.50	17
						6204	⋯	⋯	−1.36	11

This is a cut-in head

Star	V	b−y	m_1	c_1	ref	T_{eff}	log g	v_{turb}	[Fe/H]	ref
+26°2606	9.7	0.34	0.05	0.28	20,11	5980	⋯	⋯	< -2.20	19
						5950	⋯	⋯	−2.89	24
+26°3578	9.4	0.31	0.05	0.37	20,11	5830	⋯	⋯	−2.60	4
						5800	⋯	⋯	−2.62	17
						6177	⋯	⋯	−2.51	11
						6000	3.25	⋯	−2.20	22
						6140	3.50	⋯	−2.57	15

Table 3—Continued

Star	V	b−y	m_1	c_1	ref	T_{eff}	log g	v_{turb}	[Fe/H]	ref
+30°2611	9.2	0.82	0.33	0.55	2	$\cdots$	$\cdots$	$\cdots$	−1.70	2
						4400	1.80	$\cdots$	−1.70	12
						4400	0.90	1.7	−1.20	14
						4260	$\cdots$	$\cdots$	−1.55	10
+37°1458	8.9	0.44	0.07	0.22	20,11	5296	$\cdots$	$\cdots$	−2.39	11
						5420	$\cdots$	$\cdots$	−2.43	3
+58°1218	10.0	0.51	0.03	0.36	2	$\cdots$	$\cdots$	$\cdots$	−2.80	2
						5000	1.10	2.2	−2.71	14
						5000	2.20	1.8	−2.46	5
						4980	$\cdots$	$\cdots$	−2.55	10
+72°0094	10.2	0.31	0.09	0.26	12	6160	$\cdots$	$\cdots$	−1.80	19
I'm a side head:										
G5–36	10.8	0.40	0.07	0.28	20	$\cdots$	$\cdots$	$\cdots$	−1.19	21
G18–54	10.7	0.37	0.08	0.28	20	$\cdots$	$\cdots$	$\cdots$	−1.34	21
G20–08	9.9	0.36	0.05	0.25	20,11	5849	$\cdots$	$\cdots$	−2.59	11
						$\cdots$	$\cdots$	$\cdots$	−2.03	21
G20–15	10.6	0.45	0.03	0.27	20,11	5657	$\cdots$	$\cdots$	−2.00	11
						6020	$\cdots$	$\cdots$	−1.56	3
						$\cdots$	$\cdots$	$\cdots$	−1.58	21
G21–22	10.7	0.38	0.07	0.27	20,11	$\cdots$	$\cdots$	$\cdots$	−1.23	21
G24–03	10.5	0.36	0.06	0.27	20,11	5866	$\cdots$	$\cdots$	−1.78	11

Table 3—Continued

Star	V	b−y	m_1	c_1	ref	T_{eff}	log g	v_{turb}	[Fe/H]	ref
						$\cdots$	$\cdots$	$\cdots$	−1.70	21
G30–52	8.6	0.50	0.25	0.27	11	4757	$\cdots$	$\cdots$	−2.12	11
						4880	$\cdots$	$\cdots$	−2.14	3
G33–09	10.6	0.41	0.10	0.28	20	5575	$\cdots$	$\cdots$	−1.48	11
G66–22	10.5	0.46	0.16	0.28	11	5060	$\cdots$	$\cdots$	−1.77	3
						$\cdots$	$\cdots$	$\cdots$	−1.04	21
G90–03	10.4	0.37	0.04	0.29	20	$\cdots$	$\cdots$	$\cdots$	−2.01	21
LP 608–62[a]	10.5	0.30	0.07	0.35	11	6250	$\cdots$	$\cdots$	−2.70	4

[a]Star LP 608–62 is also known as BD+1°2341p. We will make this footnote extra long so that it extends over two lines.

References. — (1) Barbuy, Spite, & Spite 1985; (2) Bond 1980; (3) Carbon et al. 1987; (4) Hobbs & Duncan 1987; (5) Gilroy et al. 1988: (6) Gratton & Ortolani 1986; (7) Gratton & Sneden 1987; (8) Gratton & Sneden (1988); (9) Gratton & Sneden 1991; (10) Kraft et al. 1982; (11) LCL, or Laird, 1990; (12) Leep & Wallerstein 1981; (13) Luck & Bond 1981; (14) Luck & Bond 1985; (15) Magain 1987; (16) Magain 1989; (17) Peterson 1981; (18) Peterson, Kurucz, & Carney 1990; (19) RMB; (20) Schuster & Nissen 1988; (21) Schuster & Nissen 1989b; (22)

Spite et al. 1984; (23) Spite & Spite 1986; (24) Hobbs & Thorburn 1991; (25) Hobbs et al. 1991; (26) Olsen 1983.